

VELOCITY SPECTRUM FOR HIGH LATITUDES

A. Chepurnov, A. Lazarian, S. Stanimirovic, J. E. G. Peek, C. Heiles

Department of Astronomy, University of Wisconsin, Madison, US and
Department of Astronomy, University of California, Berkeley, CA 94720

Draft version July 4, 2019

ABSTRACT

In this paper we present results of the statistical analysis of high-latitude HI turbulence in the Milky Way. We have observed HI in the 21 cm line, obtained with the Arecibo L-Band Feed Array (ALFA) receiver at the Arecibo radio telescope. For restoration of velocity statistics we have used the Velocity Coordinate Spectrum (VCS) technique, as at the moment it is the only technique accounting for convergence of lines of sight. In our analysis we have used direct fitting of the VCS model, as its asymptotic regimes are not available with Arecibo resolution and given the restrictions from thermal smearing of the turbulent line. We have obtained a velocity spectral index 3.90 ± 0.09 , an injection scale of 105 pc and an HI temperature of 127 K. The spectral index is steeper than a Kolmogorov index and can be interpreted as ‘Shock-type’.

Subject headings:

1. INTRODUCTION

Galactic interstellar medium (ISM) is turbulent over a very wide range of spatial scales (Deshpande et al. 2000, Dickey et al. 2001, Elmegreen & Scalo 2004). This turbulence is a crucial parameter for understanding many astrophysical processes such as star formation, heat transfer, existence and evolution of ISM phases, cloud structure and dynamics, and cloud formation and destruction.

One of the main approaches for characterizing the ISM turbulence is based on using statistical descriptors. Many quantitative statistical techniques for analyzing spectral-line data cubes have been developed: the Principal Component Analysis (Heyer & Schloerb (1997)), the Spectral Correlation Function and the Spatial Power Spectrum (Rosolowsky et al. 1999), velocity centroids etc. These tools investigate intensity fluctuations in spectral-line data cubes (position-position-velocity or PPV). However, relating the fluctuations of intensity in the PPV domain with the underlying 3-D velocity and density statistics is a problem that has been only recently addressed. In some cases it required introducing a new technique, such as Velocity Channel Analysis (Lazarian & Pogosyan 2000), or modifying an existing one (Lazarian & Esquivel 2003, Brunt & Heyer 2002, Padoan, Goodman & Juvela 2003).

In this paper we apply a new statistical technique, the Velocity Coordinate Spectrum (VCS), developed in Lazarian & Pogosyan (2000), Lazarian & Pogosyan (2006) and Chepurnov & Lazarian (2007), on high-latitude HI observations obtained with the Arecibo radio telescope as a part of the all-sky survey undertaken by GALFA. GALFA is a consortium for Galactic studies with the Arecibo L-band Feed Array (ALFA). The survey specifications and strategy are described in Stanimirovic et al. (2006). GALFA datasets have high spatial and velocity dynamic range and offer the perfect opportunity for testing the VCS technique, which is at the moment the only tool accounting for convergence of lines of sight within the emitting medium.

The structure of this paper is organized as follows. In

Sect. 2 we describe briefly the HI data used in this paper. In Sect. 3 we review the VCS technique and address several important issues that need to be considered before applying VCS to HI data. In Sect. 4 we describe the fitting procedure. The overview of our results is provided in Sect. 5.

2. HI DATA

We observed a region of sky 16.7 square degrees centered on $\alpha = 2^{\text{h}}15^{\text{m}}$, $\delta = +9^{\circ}30'$ in May and June of 2005 with Arecibo’s ALFA receiver and the GALSPECT spectrometer. ALFA is a 7-element focal-plane array primarily designed for 21-cm observations. GALSPECT is a special-purpose spectrometer for Galactic science with ALFA. GALSPECT has a spectral resolution of 0.18 km s^{-1} , and a fixed bandwidth of 1380 km s^{-1} . Each of the 7 beams of ALFA has a 3.35 arcminute FWHM beam width with a beam ellipticity of 0.2 . The region contains much low-velocity, high-latitude Galactic HI, as well as a sub-complex of Very High Velocity Clouds whose analysis is detailed in Peek et al. (2007). The region was observed in a ‘basket-weave’ or meridian-nodding mode, interlacing scans from day to day.

The typical data reduction procedure is described in Stanimirovic et al. (2006) and in Peek et al. (2007). The final data cube was at the end scaled to the equivalent region in the Leiden-Dwingeloo Survey (LDS) for a single, overall gain calibration Hartmann & Burton (1997).

ALFA’s pixels are known to have asymmetric first side-lobes, as well as significant stray radiation, i.e. unmasked, distant side-lobes. These can contaminate the data slightly (between 50% and 70% of the flux is in the main beam, 10% to 20% is in the first side-lobe and 20% to 30% is in stray radiation, depending upon which ALFA pixel is measured¹). We do not attempt to correct for these effects, though we have yet to see any qualitative effects on the maps, such as echoing or visible beam patterns. Unpublished work by Carl Heiles and

¹ see C. Heiles, 2004, www2.naic.edu=alfa=memos=alfa_bm2.pdf

Tom Troland leads us to believe that the stray radiation does not come from large angular distances from the main beam. This information is corroborated by the fact that the LDS spectra are quite consistent with our observed spectra, once scaled – if much of the flux came from sidelobes more distant than 36° , the spectra would look dissimilar.

There are two emitting HI structures within the original $16^\circ \times 7^\circ$ map with a relative velocity of 8.2 km s^{-1} (see Fig. 1). The weaker and more compact one was clipped out in angular coordinates to avoid interference. The remaining region is $7^\circ \times 7^\circ$ square centered at the Galactic coordinates $l = 151^\circ$, $b = 49^\circ$.

3. THE VCS TECHNIQUE

Unlike other techniques for restoring velocity statistics from spectral-line data cubes, such as VCA or Velocity Centroids, VCS relies exclusively on information along the velocity coordinate. Other dimensions of the PPV data cube are used for improving statistics. The VCS technique uses the power spectrum calculated along the velocity axis, P_1 . The behavior of P_1 predicted by the analytic theory is compared with the measured P_1 to recover the underlying 3-d turbulent properties.

When applying the VCS technique, we need to account for several factors: the observational geometry, thermal smoothening and the effects of angular resolution.

The behavior of P_1 depends on the observational geometry. This dependence is through the geometric term, which is an autoconvolution of a 3-d sensitivity function. It accounts for the instrument beam and for the shape and location of an observed structure. This effect is mixed up with the velocity statistics (see Eq. [3]), therefore we need to know about the geometry to separate them.

For our case the observed turbulent structure is enough near and accounting for convergence of lines of sight within the beam is necessary. To simplify our model we assume that the extent of the observed structure along the line of sight is much greater than the distance to it, i.e. that the pure regime of crossing LoS. takes place².

Our analysis is also limited by smoothening of the spectral line by HI thermal line broadening. For small Mach numbers it can reduce available dynamical range over k_v (Fourier counterpart of velocity) and make restoration of velocity statistics problematic. For larger Mach numbers we can also estimate the temperature of emitting medium.

It is important to note that P_1 nontrivially depends on the angular resolution, which we can degrade during the processing of the data. Fitting of our model to such multi-resolution data increases reliability of obtained velocity statistics and provides additional test of the model relevance.

We describe here the main facts needed for our calculations (for more details see Chepurmov & Lazarian 2007).

3.1. Spectral line

Our analysis is based on the following expression for a spectral line intensity, measured at velocity v_0 and given

² we define it as an observational geometry, where the emitting structure, whose boundaries are defined by w^* in Eq. [2], overlaps the point of observation.

beam position:

$$S(v_0) = \int w(\mathbf{r}) d\mathbf{r} \int f(v_r(\mathbf{r}) + v_r^{\text{reg}}(\mathbf{r}) - v_0) : (1)$$

Here f is normalized emissivity, f is convolution between channel sensitivity function and Maxwellian distribution, defined by temperature of emitting medium, v_r is a turbulent velocity, v_r^{reg} is a regular velocity due to Galactic rotation, and w is a window function defined as follows:

$$w(\mathbf{r}) = \frac{1}{r^2} w_b(\mathbf{r}; \mathbf{r}_0) w^*(\mathbf{r}); \quad (2)$$

where w_b is an instrument beam, w^* is a window function defining borders of the observed object.

3.2. Spectrum along velocity coordinate

To calculate the power spectrum P_1 , we Fourier-transform S and average its squared modulus:

$$P_1(k_v) = \int_D \int_E \mathcal{E}(k_v) \mathcal{E}^*(k_v) = \int_D \int_E \mathcal{E}^2(k_v) w_a(\mathbf{r}) d\mathbf{r} \int_C w^*(\mathbf{r}) \exp\left(\frac{k_v^2}{2} D_z(\mathbf{r}) - ik_v b z\right); \quad (3)$$

where the geometric term w_a is defined as follows:

$$w_a(\mathbf{r}) = \int_D \int_E w(\mathbf{r}^0) w(\mathbf{r}^0 + \mathbf{r}) d\mathbf{r}^0 \quad (4)$$

and D_z is a velocity structure tensor projection:

$$D_z(\mathbf{r}, \mathbf{r}^0) = \int_D \int_E (v_z(\mathbf{r}) - v_z(\mathbf{r}^0))^2 : \quad (5)$$

Expression [3] is true under the following assumptions: (1) the fields involved are homogeneous, (2) the velocity is Gaussian, (3) the absorption effects are negligible³, (4) the beam width is small enough to neglect the difference between v_x and v_z , and (5) $v_z^{\text{reg}}(\mathbf{r})$ depends only on z and admits a linear approximation with angular coefficient b ⁴.

In our case w^* is non-zero at $\mathbf{r} = 0$ and therefore the singularity in Eq. [2] is relevant. This determines the behavior of P_1 in the regime of crossing lines of sight.

It can be shown, that if we assume a Gaussian beam with a radius r_0 , correspondent w_a can be reduced to the following form:

$$w_a(\mathbf{r}) = \frac{1}{2} \int_0^z \frac{w^*(z^0) w^*(z^0 + \mathbf{j} \cdot \mathbf{j})}{z^2 + (z^0 + \mathbf{j} \cdot \mathbf{j})^2} \exp\left(\frac{R^2}{2(z^2 + (z^0 + \mathbf{j} \cdot \mathbf{j})^2)}\right) dz^0; \quad (6)$$

where w^* can be expressed with:

$$w^*(z) = \begin{cases} 1; & z \in [0; z_{\text{edge}}] \\ 0; & z \notin [0; z_{\text{edge}}] \end{cases} \quad (7)$$

and z_{edge} is a layer thickness in given direction.

³ In this case the analysis is much simpler as we use the Fourier space. Absorption effects can be described only in real space, which implies using of structure functions instead, see Lazarian & Pogosyan (2006)

⁴ Hereafter we will set $b = 0$, as the regular velocity shear is not relevant for the selected site

3.3. Velocity structure tensor

We need now to express D_z through the velocity spectrum. If we consider $\mathbf{v}(\mathbf{x})$ solenoidal with power-law power spectrum having cutoff at large scales, the latter can be written in as follows (see, for example, Lesieur 1991):

$$F_{ij}(\mathbf{k}) = \frac{V_0^2}{k^\nu} e^{-\frac{k_0^2}{k^2}} \delta_{ij} \frac{k_i k_j}{k^2} \quad (8)$$

where V_0^2 is the velocity power spectrum amplitude, ν is the velocity spectral index, $k_0 = 2\pi/L_v$ is the cutoff wavevector, bound with the injection scale L_v . Then D_z can be represented as follows:

$$D_z(\mathbf{x}) = 2 \int d\mathbf{k} (1 - e^{i\mathbf{k}\cdot\mathbf{x}}) \hat{z}_i \hat{z}_j F_{ij}(\mathbf{k}) \quad (9)$$

3.4. Asymptotics

There are two asymptotic regimes of the theoretical spectrum [3], depending on the beam width, see Fig. 3. For high resolution mode (where k_v is less than the wavenumber corresponding to velocity variance on the beam scale in the middle of emitting layer) the slope of P_1 is $2 - (\nu - 3)$, otherwise, in low resolution mode⁵ it is $4 - (\nu - 3)$. Both cases require k_v big enough to ignore saturation of D_z in Eq. [3]. Calculations show that this condition is not met for our data⁶.

3.5. P_1 model for fitting

As we do not have pure asymptotic regimes, we have to determine unknown parameters by direct fitting of predicted P_1 curves to the observational data. To make their calculation simpler we factor out the emissivity term from Eq. [3], as it is weaker than the singular w_a and the exponent term with k_v . This results in the following expression for P_1 :

$$P_{1,\text{model}}(k_v) = \int d\mathbf{x} w_a(\mathbf{x}) \exp\left(-\frac{k_v^2}{2} D_z(\mathbf{x})\right) + N_0; \quad (10)$$

where P_0 is the spectrum amplitude and N_0 is a constant, depending on the detector white noise and the resolution.

The fitting parameters, other than P_0 , reside in the structure function D_z (velocity parameters) and effective channel sensitivity f (HI temperature). N_0 is estimated directly from observational data.

4. APPLICATION TO THE HI DATA

We minimize the sum of squared deviations between real and model P_1 in log-log coordinates. This is done in Mathematica with the function FindMinimum, which implements the algorithm of steepest descent. It yields

⁵ we assume steep density spectrum for the both cases

⁶ the model P_1 can not be fitted to the real one for ν directly recounted from the slope of P_1 , in assumption that the high-resolution regime takes place.

an estimation of the model parameters: velocity spectral index ν , injection scale L_v , velocity spectrum amplitude V_0 , VCS amplitude P_0 and HI temperature T . Fitting has been performed for the P_1 data, calculated for degraded resolutions of 0.125, 0.250 and 0.500. The results are presented on Fig. 2.

While the fitting is satisfactory, there is some systematic error. For the highest resolution the theoretical curve is systematically below the data, for the lowest resolution the theoretical curve is systematically above the data. This is to say that P_1 drops with increase of beam width somewhat faster than expected. We conjecture that the observation point is slightly outside of the emitting structure, which leads to cutting off the singularity of the window function (Eq. [2]). The latter can cause the slope of P_1 to be steeper than expected for the same original ν , which can cause the effect we observe⁷.

Thus we probably have the case intermediate between pure crossing *l.o.s.* regime and the parallel *l.o.s.* one, but much more like the crossing *l.o.s.* one (for the latter case deviation is 50 times smaller). However, correspondent error is tangible only with respect to P_1 error bars, which are relatively small.

For calculation of statistical error of the velocity spectral index we deviate it from optimum and let the other parameters compensate the correspondent deviation of our target function. This gives us some other model curves, deviating from the optimum as well. We interpret the mean squared deviation between these two sets of model curves, normalized by variances of respective measured P_1 values, as squared normalized deviation of the parameter itself. As we know its absolute deviation, we get the variance. By taking as a reference point the fitted model instead of the data, we separate the effect of deviation from the influence of the systematic error and statistical scattering of data.

5. SUMMARY

Applying the VCS technique to the 7.7 site centered at $l = 151$, $b = 49$ we have determined the following HI parameters: velocity spectral index $\nu = 3.90 \pm 0.09$, injection scale $L_v = 105 \text{ pc}$ and temperature $T = 127 \text{ K}$. The derived Mach number is 7.6. The spectral index is steeper than the Kolmogorov one, so we have a shock-type velocity spectrum.

It has been shown, that the observational geometry is close to the case of crossing *l.o.s.*, i.e. that the distance to the emitting structure is much smaller than its extent over line of sight.

This is the first attempt of trying the VCS on real data. It shows, that VCS can be used even if asymptotic regimes are not achieved, which increases its field of application.

⁷ see Chepurinov & Lazarian (2007) for the discussion of the influence of singularity in the expression for P_1 on its spectral index

REFERENCES

- Burnt, C. M., Heyer, M. H., ApJ, 566, 276 (2002)
 Chepurinov, A., Lazarian, A., submitted to ApJ, (2007)
 Deshpande, A. A., Dwarakanath, K. S., Goss, W. M., ApJ, 543, 227 (2000)

- Dickey, J. M., McClure-Grieths, N. M., Stanimirovic, S., Gaensler, B. M., Green, A. J., *ApJ*, 561, 264 (2001)
- Elmegreen, B. & Scalco, J., *ARA & A*, 42, 211 (2004)
- Esquivel, A. & Lazarian, A., *ApJ*, 784, 320 (2005)
- Hartmann, D., & Burton, W. B., *Atlas of Galactic Neutral Hydrogen*, (Cambridge: Cambridge University Press) (1997)
- Heyer, M. H., Schilber, F. P., *ApJ*, 475, 173 (1997)
- Lazarian, A., Esquivel, A., *ApJ*, L37 (2003)
- Lazarian, A., Pogosyan, D., *ApJ*, in press, astro-ph/0511248 (2006)
- Lazarian, A., Pogosyan, D., *ApJ*, 537, 720 (2000)
- M. Lesieur, *Turbulence in fluids*, Kluwer Academic Publishers, (1991)
- Padoan, P., Goodman, A. A., Juvela, M., *ApJ*, 588, 881 (2003)
- Peek, J. E. G., Putnam, M. E., McKee, C. F., Heiles, C., Stanimirovic, S., *ApJ*, in press (2007)
- Rosolowsky, E. W., Goodman, A. A., Wilner, D. J., & Williams, J. P., *ApJ*, 524, 887 (1999)
- Stanimirovic, S., Putnam, M. E., Heiles, C., Peek, J. E. G., Goldsmith, P. F., Koo, B.-C., Kroo, M., Lazarian, A., Lee, J.-J., Mook, J. M., Muller, E., Pandian, J. D., Parsons, A., Tang, Y., & Werthimer, D., *ApJ*, in press (2006)

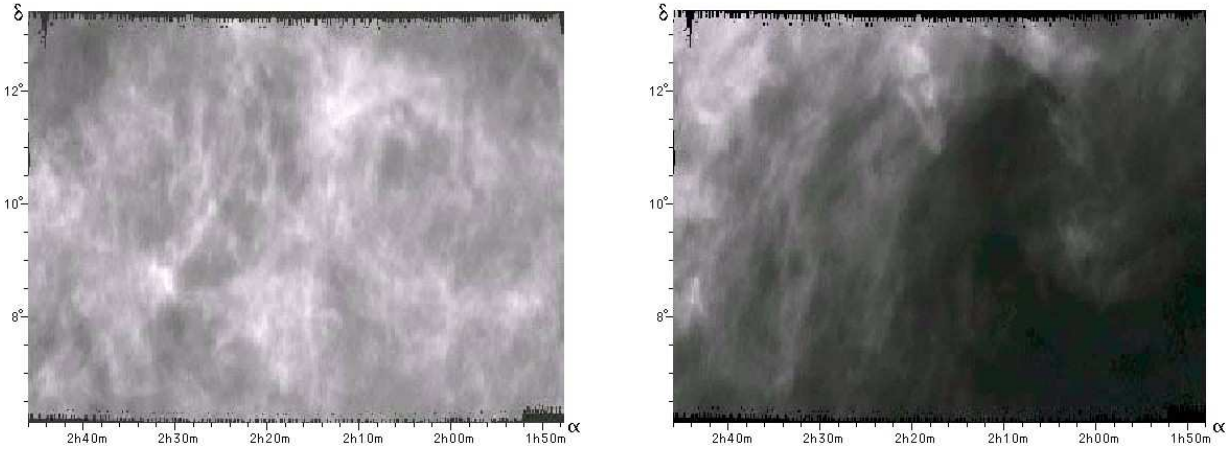


Fig. 1. | Maps of the two emitting lines, corresponding to the entire observed region. The main turbulent line (left) is contaminated with some bright feature (right), which can distort P_1 . To avoid this, only the right half of this PPV data cube has been used, which approximately corresponds to the $7^\circ \times 7^\circ$ area centered at $l = 151^\circ$, $b = -49^\circ$. The separation between lines is 8.2 km/s .

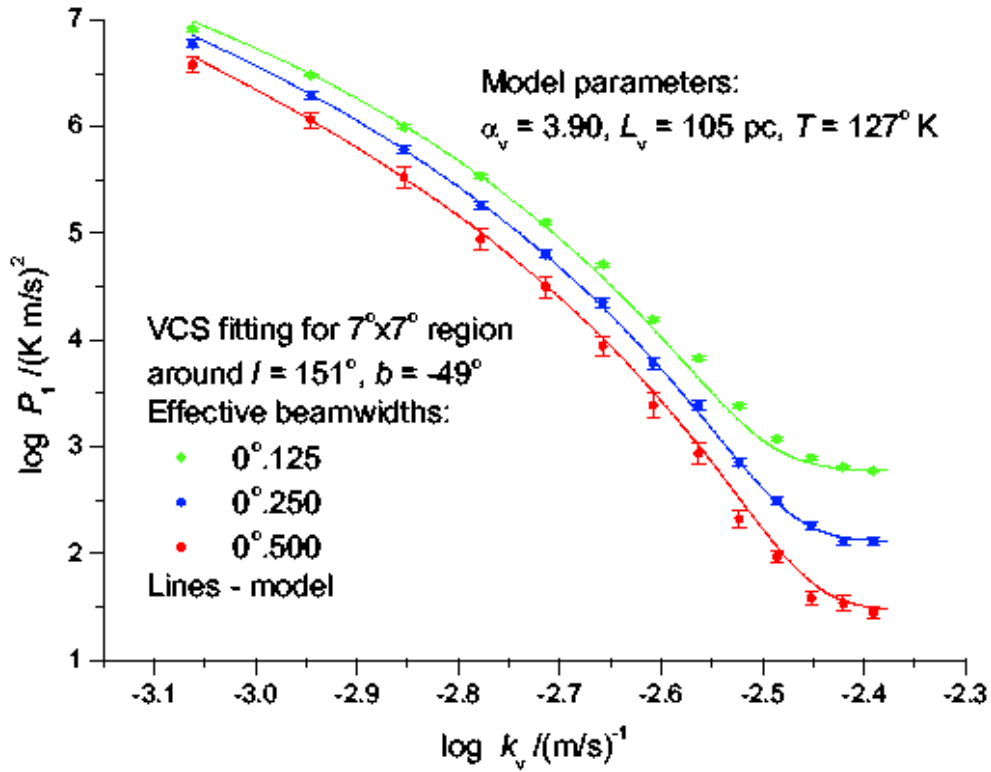


Fig. 2. | Fitting of model VCS spectra to P_1 data, obtained from GALFA data cube for different effective resolutions. The regime is non-asymptotic for all resolutions.

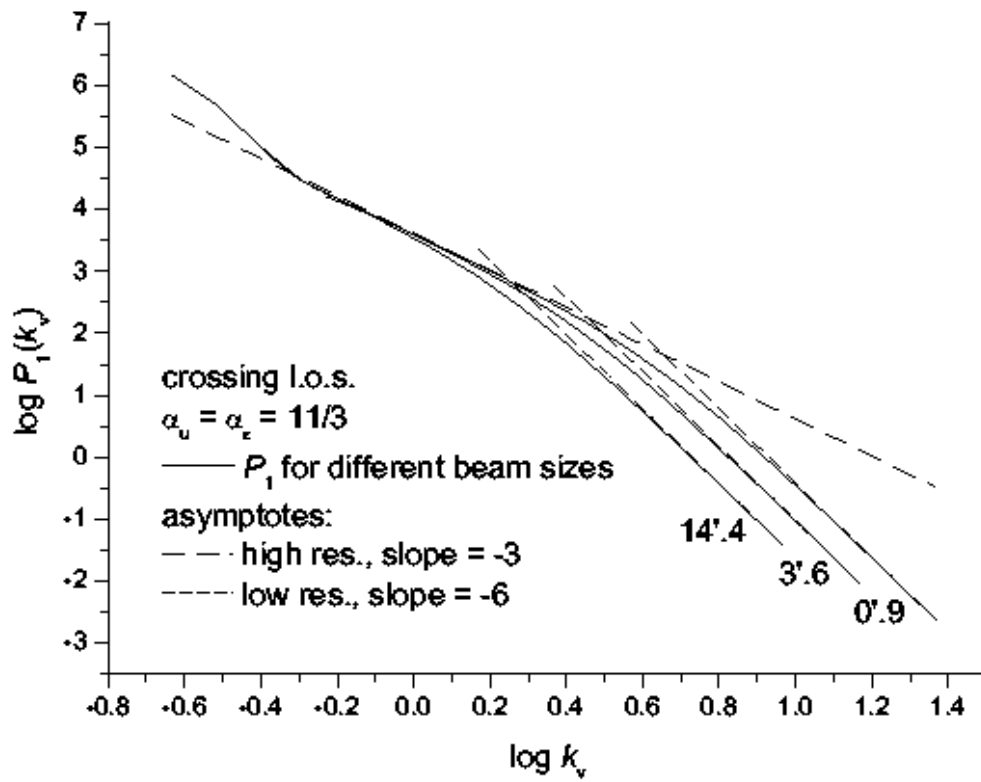


Fig. 3. | Direct calculation of P_1 for crossing lines of sight geometry. The dynamical range over k_v is big enough to observe both asymptotic regimes.